Sugi, J Material Sci Eng 2017, 6:5
DOI: 10.4172/2169-0022.1000386

Journal of Material Sciences & Engineering

Review Article Open Access

Evidence for the Essential Role of Myosin Subfragment-2 in Muscle Contraction: Functional Communication between Myosin Head and Subfragment-2

Sugi H*

Department of Physiology, School of Medicine, Teikyo University, Tokyo, Japan

Abstract

In 1971, Harrington et al. put forward a hypothesis, in which helix-coil transition in the hinge region of myosin subfragment-2 (S-2) contributes to muscle contraction. The helix-coil transition hypothesis has been, however, ignored by muscle investigators over many years. In 1992, we worked with him to examine the effect of polyclonal antibody to myosin subfragment-2 (anti-S-2 antibody), and found that the antibody eliminated Ca^{2+}-activated isometric force generation of skinned vertebrate muscle fibers without affecting MgATPase activity. Further studies using the same antibody indicated functional communication between myosin head and myosin S-2, including regulation of binding strength between myosin head and actin filament during Ca^{2+}-activated contraction in vertebrate muscle fibers. These findings indicate that the swinging lever arm hypothesis, in which muscle contraction results from active rotation of myosin head converter domain, is incomplete because it ignores of the role of myosin S-2. Much more experimental work is necessary to reach full understanding of muscle contraction mechanism at the molecular level.

Highlights

- Harrington's helix-coil transition theory of muscle contraction is explained.
- Using the gas environmental chamber attached to electron microscope, we observed marked ATP-induced myosin head movement in hydrated myosin-paramyosin core complex filaments, which is only accounted for by the helix-coil transition taking place in myosin subfragment-2 region.
- We obtained experimental evidence for the functional communication between myosin head (myosin subfragment-1) and subfragment-2, including the regulation of binding strength of myosin head with actin filament.
- We emphasize the essential role of subfragment-2 in producing muscle contraction, which has been totally ignored in the current swinging lever arm hypothesis appearing in every textbooks.

Keywords: Muscle contraction; Myosin subfragment-2; Gas environmental chamber; ATP-induced myosin head movement; Muscle force generation; Muscle ATPase activity; Actin-myosin binding strength

Theory

Structural basis of muscle contraction

In 1954, Hugh E Huxley and Jean Hanson made a monumental discovery that muscle contraction results from relative sliding between actin and myosin filaments, which in turn is produced by cyclic attachment and detachment between myosin heads extending from myosin filaments and corresponding sites in actin filaments [1]. As shown in Figure 1A, a myosin molecule (MW, 450,000) consists of two pear-shaped heads (myosin subfragment-1) and a rod of 156 nm long, and is split enzymatically into two parts: (1) the rod of 113 nm long (light meromyosin, LMM) and (2) the rest of myosin molecule including two heads and a rod of 43 nm long (heavy meromyosin, HMM). The HMM can be further split into two separate heads (subfragment-1, S1) and a rod (subfragment-2, S-2). In myosin filaments, LMM aggregates to form filament backbone, which is polarized in opposite directions across the filament central region (bare region, as illustrated in Figure 1B). The S-2 rod serves as a hinge between the S-1 heads and the filament backbone, so that the S-1 heads can swing away from the filament to interact with actin filaments. The axial separation between adjacent pairs of S-1 heads is 14.3 nm.

Actin filaments consists primarily of two helical strands of globular actin monomers (MW, 41,700), which are wound around each other with a pitch of 35.5 nm. The axial separation of actin monomers in actin filaments is 5.46 nm (Figure 1C). In vertebrate muscle, actin filaments also contain two regulatory proteins, tropomyosin and troponin. In relaxed muscle, interaction between S-1 heads and actin filaments is inhibited sterically by tropomyosin, When Ca^{2+}, released from the sarcoplasmic reticulum, binds with troponin; it removes the inhibitory effect of tropomyosin to start cyclic actin-myosin interaction producing sliding between actin and myosin filaments, i.e. muscle contraction. In skinned muscle fibers, in which the surface membrane is removed by treatment with glycerol, the fibers can be activated to contract by externally applied Ca^{2+}. Figure 1D shows longitudinal arrangement of actin (thin) and myosin (thick) filaments in muscle. Actin filaments

***Corresponding author:** Haruo Sugi, Department of Physiology, School of Medicine, Teikyo University, Tokyo, Japan, Tel/Fax: +81 484 78 4079; E-mail: sugi@kyf.biglobe.ne.jp

Received October 03, 2017; **Accepted** October 20, 2017; **Published** October 31, 2017

Citation: Sugi H (2017) Evidence for the Essential Role of Myosin Subfragment-2 in Muscle Contraction: Functional Communication between Myosin Head and Subfragment-2. J Material Sci Eng 6: 386. doi: 10.4172/2169-0022.1000386

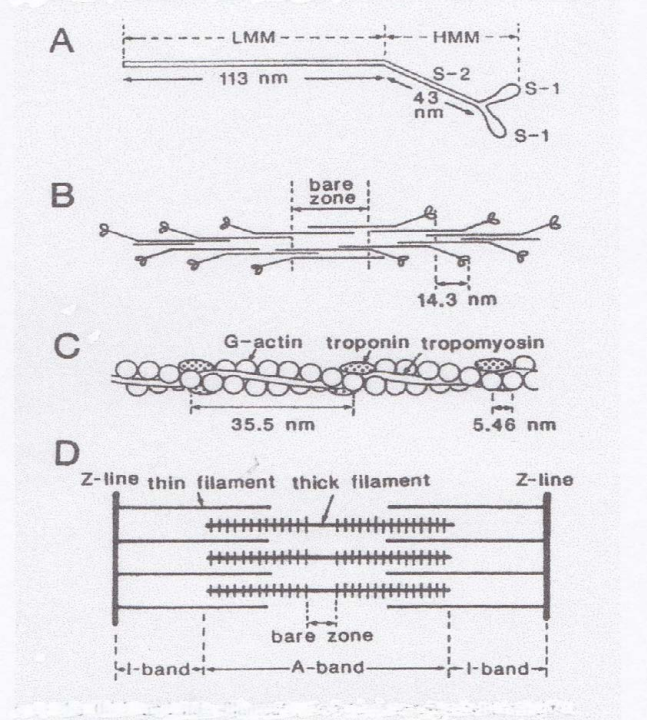

Figure 1: Structure of myosin and actin filaments and their arrangement in a sarcomere. (A) Structure of myosin molecule. (B) Polymerization of myosin molecules into myosin filament. (C) Structure of actin filament. (D) Arrangement of actin (thin) and myosin (thick) filaments in a sarcomere.

extend in either direction from Z-line to penetrate in between myosin filament arrays, which are located central in each sarcomere, i.e. the structure between two adjacent Z-lines to serve as structural and functional unit of muscle. In each sarcomere, the region containing only actin (thin) filaments is called the I-band, while the region containing both actin (thin) and myosin (thick) filaments is called the A-band. When a muscle is activated to contract, relative sliding between actin and myosin filaments, coupled with ATP hydrolysis, occurs in such a way that actin filaments are pulled into myosin filament arrays, while the length of actin and myosin filaments remains constant.

Attachment-detachment cycle between myosin heads and actin filaments

After the establishment of the sliding filament mechanism, the remaining problem is "what makes the filaments slide?". Both the actin binding sites and the ATPase activity are localized in S-1 heads, which will hereafter be called myosin heads. It is generally believed that myosin heads play a major role in muscle contraction coupled with ATP hydrolysis. Figure 2 illustrates an idea that occurred to Hugh Huxley as soon as he discovered the myofilament arrays in muscle electron microscopically [2]. As the longitudinal periodicity of myosin heads is different from that of myosin-binding sites in actin filaments, their interaction takes place asynchronously. As shown in the upper diagram, a myosin head (located in the left) extending from thick myosin filament first attaches to a myosin binding site in thin actin filament. The attached myosin head then changes its configuration to produce a unitary sliding between actin and myosin filaments; in such a way that actin filament is moved in between myosin filament arrays (middle diagram). The change in configuration of myosin head corresponds to myosin head power stroke to produce nitary sliding

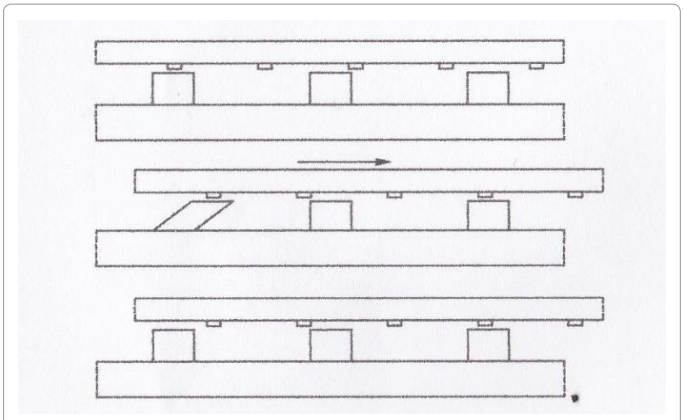

Figure 2: Diagrams showing the attachment-detachment cycle between myosin heads extending from myosin filaments and myosin-binding sites in actin filaments. For explanations, see text [2].

between actin and myosin filaments. After completion of power stroke, myosin heads detaches from actin filament, and returns to its original configuration (lower diagram). The return of myosin head to its original configuration corresponds to myosin head recovery stroke. Thus, myofilament sliding goes on by repeated asynchronous attachment-detachment between myosin heads and actin filaments. Considering the dimension of myofilament-lattice, the amplitude of myosin head power and recovery strokes may not much exceed ~10 nm [3].

Muscle is a machine converting chemical energy of ATP hydrolysis into mechanical work. The only substrate for myosin head ATPase is MgATP [4].

For biochemical experiments on myosin head ATPase reaction steps, HMM or S-1 in solution is used. Their ATPase activity is very slow, but increases ~200 fold when actin filaments are added. This phenomenon is called actin-activation of myosin ATPase activity, and has been studied intensively by many investigators by quickly mixing HMM or S-1 solution with actin filament solution and measuring release of ATP hydrolysis product, Pi and ADP. It should be noted, however, that (1) HMM or S-1 concentration in the actomyosin solution is kept to be a few micromolar, compared to myosin head concentration in muscle fibers of 100-200 micromolar, and (2) that the 3D miofilment-lattice structure is completely lost in actomyosin solution. Nevertheless, the most plausible sequence of actomyosin ATPase reaction steps, known as the Lymn-Taylor scheme [5], has been presented. As shown in Figure 3, this scheme contains attachment of myosin heads to, and their detachment from, actin filament. (1) In relaxed muscle (pCa in the myoplasm, >9), myosin heads (M) are in the state of complex M-ADP-Pi and are detached from actin filament (A). (2) When muscle is made to contract by increasing the myoplasmic pCa to 4, M-ADP-Pi first bind with A weakly (weak A-M binding), as M-ADP-Pi+A → A-M-ADP-Pi. (3) When A-M-ADP-Pi releases Pi, M binds strongly with A (weak to strong A-M binding transition). (4) M performs power stroke, coupled with release of Pi and ADP, as AM-ADP.Pi → A-M; ADP+Pi, while strongly bound with A. (5) At the end of power stroke, M remains strongly bound with A to form rigor complex A-M. When next ATP comes to bind with M, M detaches from A, as A-M+ATP → A+M-ATP. (6) M performs recovery stroke to return to the initial configuration coupled with ATP hydrolysis, as M-ATP → M-ADP-Pi, and again attaches to A. Figure 4 is a comprehensive diagrams illustrating the attachment-detachment cycle between myosin head (M) and actin filament (A) in a realistic

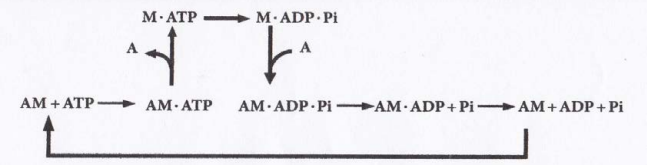

Figure 3: Lymn-Taylor scheme of actomyosin ATPase reaction steps. Note that myosin head (M) repeats attachment to, and detachment fro, actin filament (A) [5].

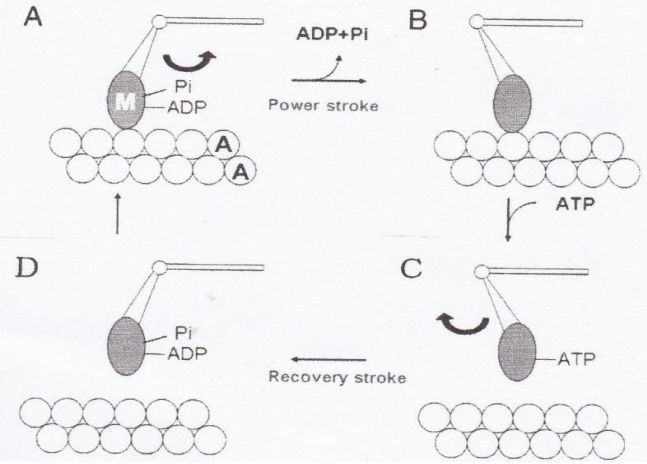

Figure 4: Diagrams illustrating the attachment-detachment cycle between myosin head (M) and actin filament (A). For explanations, see text [10].

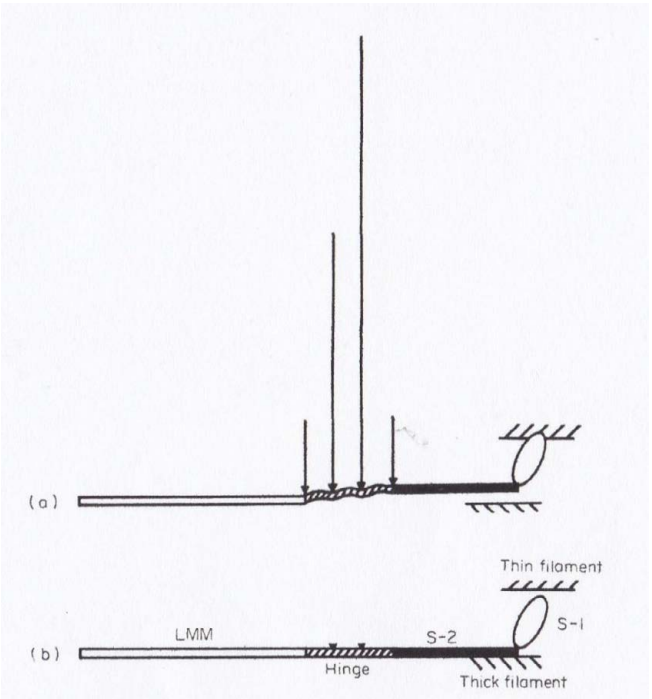

Figure 5: Diagrammatic representation illustrating chymotryptic cleavage in myosin S-2 region. Normalized cleavage rate constants are compared between Ca^{2+}-activated (a) and relaxed and rigor (b) muscle fibers. Length of vertical arrows is proportional to the rate constants [7].

manner. Chemical energy derived from ATP hydrolysis is stored in myosin heads in the form of M-ADP-Pi during the recovery stroke, to be used as mechanical energy producing power stroke after attachment to A. To repeat attachment-detachment cycle, power and recovery strokes should be the same in amplitude, and opposite in direction. Although extensive studies including chemical probe experiments and time-resolved X-ray diffraction experiments were hitherto made to record movement of myosin heads coupled with ATP hydrolysis, no definite results were obtained until 1997 when we first succeeded in recording ATP-induced myosin head movement in hydrated, living myosin filaments using the gas environmental chamber attached to an electron microscope [6].

Proposal of the helix-coil transition theory by Harrington

William F Harrington was a prominent polymer scientist, and got interested in the mechanism of muscle contraction. Reflecting his research carrier, he focused attention on the hinge region of myosin S-2, by which myosin heads can move towards actin filaments. To detect possible structural changes in the hinge region in myosin S-2, he used the enzyme probe method, in which the rate of splitting of S-2 hinge region by proteolytic enzyme, chymotrypsin was compared between skinned muscle fibers in relaxed, contracting and rigor states. He found that the S-2 hinge region was split rapidly by chymotrypsin in Ca^{2+}-activated, contracting fibers, while the S-2 hinge region in relaxed and rigor fibers was not readily split by chymotrypsin (Figure 5) [7], indicating some structural changes in the S-2 hinge region in Ca^{2+}-activated fibers. Based on this and other experiments, Harrington proposed a contraction model shown in Figure 6, which resembles that in Figure 4, except that myosin head power and recovery strokes are replaced by helix-coil transition (or melting) of S-2 hinge region [7].

ATP-induced movement of individual myosin heads in hydrated myosin-paramyosin core complex filaments recorded using the gas environmental chamber

In this section, we will describe our early electron microscopic experiments using the gas environmental chamber [6], since the results obtained seem to be consistent with shortening of S-2 region predicted by Harrington. As illustrated diagrammatically in Figure 7, the gas environmental chamber (will hereafter be called EC) is a cylindrical compartment (diameter, 2 mm; height, 0.8 mm) with upper and lower windows to pass electron beam. Each window is covered with a thin carbon sealing film (thickness, 15-20 nm) held on a copper grid with nine apertures (diameter, 0.1 mm for each). The carbon sealing film can bear pressure difference up to 1 atmosphere. The biological specimen placed on the lower carbon film is kept wet by constantly circulating water vapor (pressure, 60-80 torr; temperature, 26-28°C) through the chamber. The EC contained an ATP containing microelectrode with its tip immersed in a thin layer of experimental solution, to apply ATP to the specimen ion theoretically. The EC was attached to a 200 kV transmission electron microscope (JEM 2000EX; JEOL). The material used was synthetic filament, in which rabbit skeletal muscle myosin was bund on the surface of thick paramyosin filaments obtained from molluscan catch muscle. The myosin-paramyosin core complex filaments (diameter, 50-200 nm; length, 10-30 μm) were very easy to handle. To position-mark individual myosin heads, colloidal gold particles (diameter, 15 nm; coated with protein A) were attached to myosin heads via site-directed monoclonal antibody to distal region of myosin head. Further details of the methods have been described elsewhere [8,9]. Figure 8 shows electron micrograph of myosin-

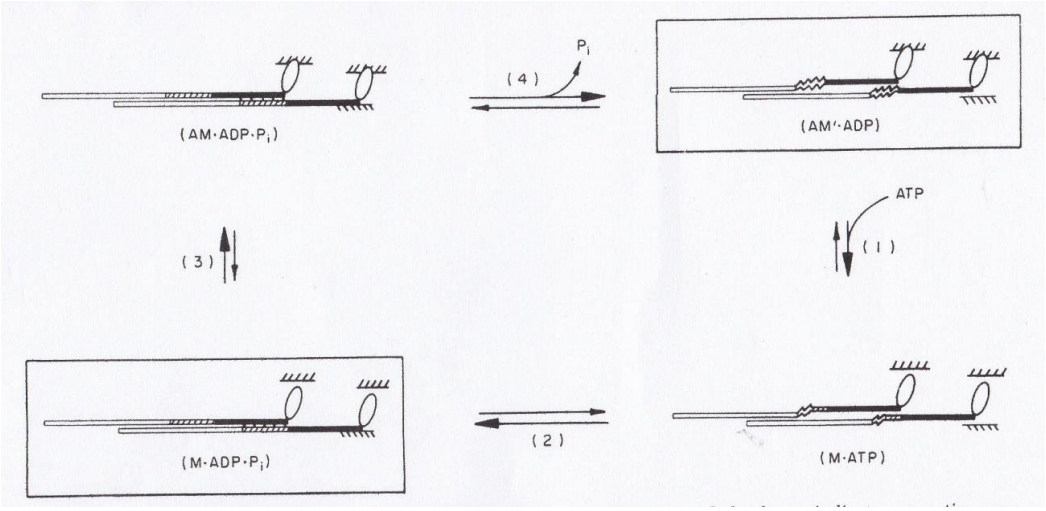

Figure 6: Schematic diagram illustrating the helix to (random) coil transition cycle occurring in myosin-S-2 hinge region proposed by Harrington [9]. Helical and random coil structures of the S-2 hinge region are expressed as straight and zig-zag shapes, respectively [7].

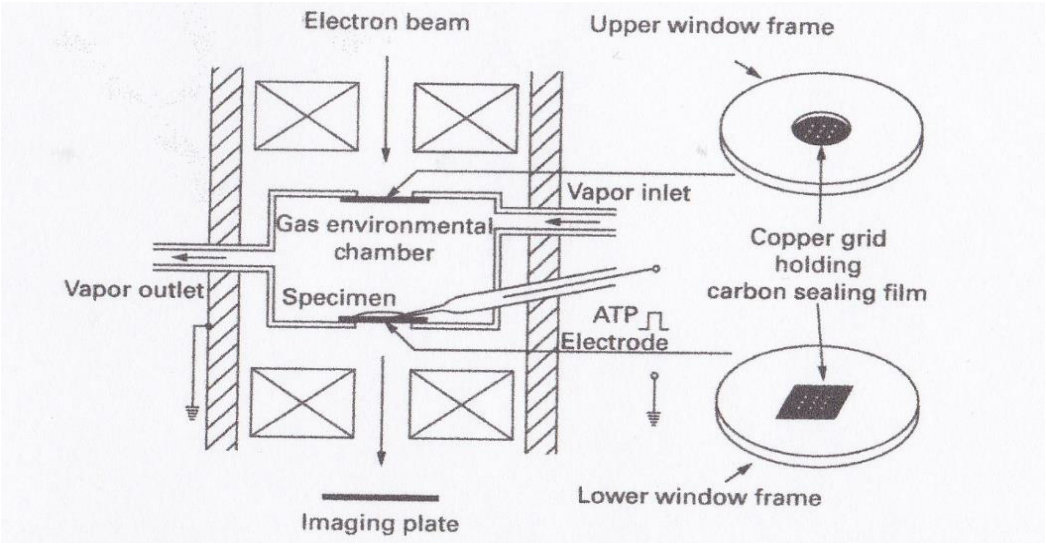

Figure 7: Diagram of the EC. Myosin filaments are placed on the lower carbon sealing film together with a thin layer of experimental solution. ATP is delivered from the ATP-containing microelectrode to the filaments. For further explanations, see text [6].

paramyosin core complex filaments with a number of gold paritcles attached to individual myosin heads.

First, we recorded filament images with an imaging plate system (magnification, 10,000X) two times at intervals of several min, and found that the position of each gold particle did not change appreciably, indicating that each myosin head undergoes thermal motion around a definite equilibrium position, so that the time-averaged mean position of individual myosin heads remains almost unchanged, as predicted by Huxley [10]. Being encouraged with this finding, we recorded the same filament images two times, one before and the other after application of ATP. As shown in Figure 9, we found that individual gold particles, i.e. individual myosin heads, moved in response to ATP in the direction parallel to the filament axis. The average amplitude of ATP-induced myosin head movement was 20 nm, a value too large to be accounted for by the movement of myosin heads. This implies that, in the complex filaments, myosin molecules tend to attach to the paramyosin filaments parallel to its long axis at their LMM region, while it's HMM region can move more or less freely. If this assumption is correct, the large amplitude of ATP-induced myosin head movement is likely to result from the helix to random coil transition occurring at the S-2 region, constituting evidence that the helix to random coil transition actually takes place under some conditions. Since the experiments were performed in the absence of actin, the observed myosin head movement is regarded to be its recovery stroke, which is believed to be the same as power stroke in amplitude and opposite in direction.

Effect of anti-S-2 antibody on isometric force production, force-velocity relation, and MgATPase activity in skinned vertebrate muscle fibers

Although Harrington's theory was unique and interesting, most muscle investigators ignored it. Nevertheless, Harrington intended to demonstrate the important role of S-2 hinge region in muscle contraction, and prepared a polyclonal antibody to S-2 hinge region (anti-S-2 antibody), and showed that the antibody reduced Ca^{2+}-

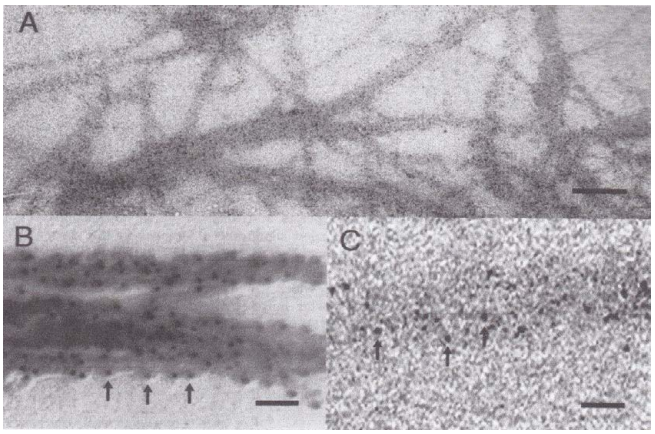

Figure 8: Images of the myosin-paramyosin core complex filaments. (A) Imaging plate record of the filaments with numerous colloidal gold particles attached to individual myosin heads. Bar 500 nm. (B) Conventional electron micrograph of negative stained filaments. Bar 100 nm. (C) Enlarged imaging plate record showing part of the filament with gold particles on it. Bar 100 nm. In B and C, gold particles are indicated by arrows [6].

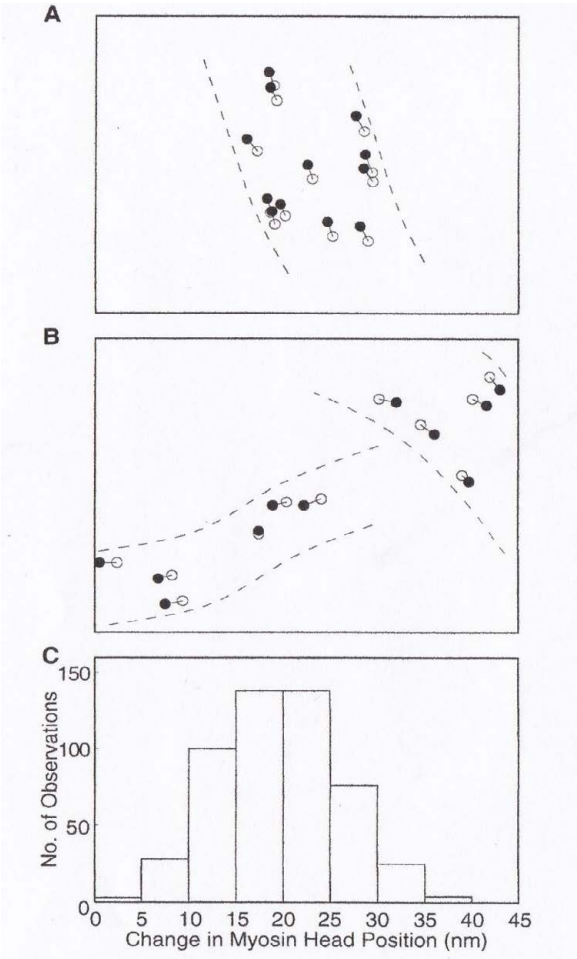

Figure 9: ATP-induced movement of individual gold particles, i.e. individual myosin heads. (A and B) Examples of changes in position of individual myosin heads. Filled and open circles (diameter, 15 nm) are drawn around the center of mass positions of each particle image before and after ATP application, respectively. (C) Histogram showing amplitude distribution of ATP-induced myosin head movement [6].

activated isomeric force generation and slowed down Ca^{2+}-activated myofibrillar shortening [11,12]. In 1992, he asked me to work together using his anti-S-2 antibody, and we made the experiments to be described later with unexpected results. At that time, he appeared to change his mind, and intended to emphasize possible communication between myosin head and subfragment-2 in regulating actin-myosin interaction producing muscle contraction, and his intension was achieved, at least in part, by the experiments described below.

Figure 10 is a typical result showing the effect of anti-S-2 antibody on Ca^{2+}-activated isometric force and Mg ATPase activity, measured by NADH fluorescence, in skinned vertebrate muscle fibers. In agreement with the report of Harringon [12], the antibody reduced isometric force in a time-dependent manner, while Mg ATPase activity remained unchanged even when isometric force was reduced to zero [13]. As shown in Figure 11, Muscle fiber stiffness, measured by applying small sinusoidal vibrations (amplitude, 0.1% of fiber slack length) decreased with decreasing isometric force, reaching zero when isometric force was reduced to zero. We also obtained the force-velocity relation of anti-S-2 treated muscle fibers by applying ramp decreases in force to isometrically contracting fibers and recording resulting fiber shortening (Figure 12). To our surprise, the force-velocity curves thus obtained showed that, despite marked reduction of steady isometric force caused by the antibody, the maximum shortening velocity Vmax remained unchanged, as shown in Figure 13. It can be seen that the force-velocity curves, obtained at various levels of reduced isometric force (Figure 13A) are shown to be identical when they are normalized with respect to the maximum steady forces (Figure 13B). When author

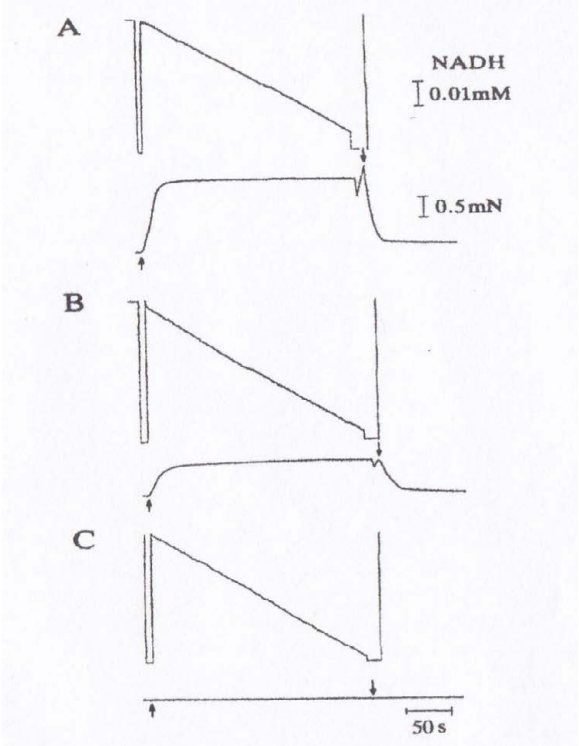

Figure 10: Simultaneous recordings of Mg ATPase activity (upper traces) and Ca^{2+}-activated isometric force development (lower traces) in skinned vertebrate muscle fibers before (A) and 100 min (B) and 150 min (C) application of anti-S-2 antibody (1.5 mg/ml). Note that the slope of ATPase records (decrease in NADH), representing the Mg ATPase activity, remains unchanged, even when the isometric force is reduced to zero. Times of application of contracting and relaxing solution are indicated by upward and downward arrows, respectively [13].

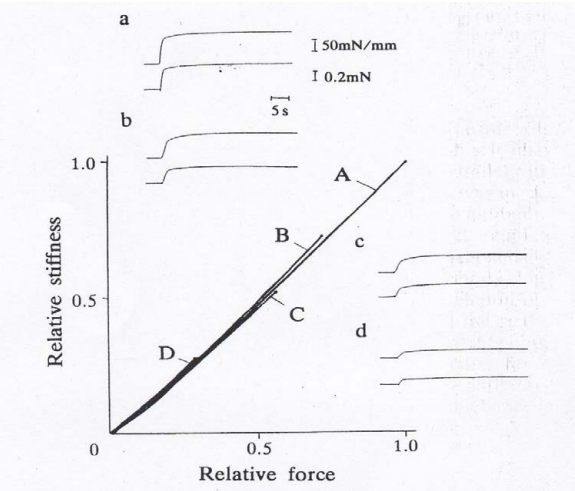

Figure 11: Relation between muscle fiber stiffness and Ca^{2+}-activated isometric force in the presence of anti-S-2 antibody (1.5 mg/ml). The stiffness versus isometric force curves A, B, C and D were obtained before, at 30, 60, and 90 min after application of antibody, respectively (Insets) [13].

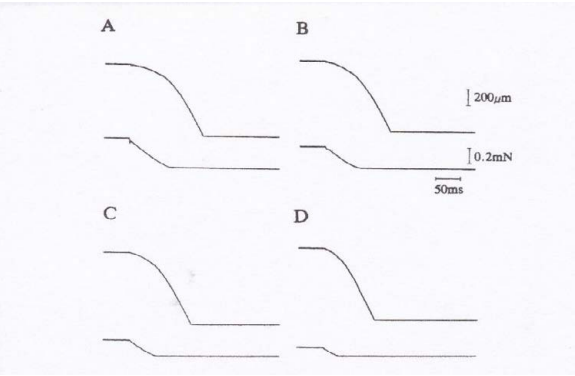

Figure 12: Changes in fiber length (upper traces) and force (lower traces) of skinned fibers in response to ramp decreases in force applied at the steady Ca^{2+}-activated isometric force before (A, control) and at 30 (B), 60 (C) and 90 min after application of anti-S-2 antibody (1.5 mg/ml) [13].

informed the results described above to Harrington, he was extremely happy with them, and stated in his mail, "This is a triumph. We can now demonstrate the fact that S-2 region can influence on myosin head-actin interface!". To our great pity, however, he suddenly passed away before the publication of our work. Reflecting his contribution to the field of polymer science and his personality, a two day-long memorial symposium was held at Johns Hopkins University, and we were selected to be the first speaker by the request of Mrs. Harrington, who knew that his husband suddenly passed away with happy feeling in mind.

Evidence that myosin S-2 regulates binding strength between myosin heads and actin filaments

As soon as we received anti-S-2 antibody from Harrington, we examined the point of attachment of the antibody in myosin molecule by observing rotary shadowed electron micrographs of the antibody (IgG)-myosin complex, and found that the antibody attached not only to S-2 hinge region, but also uniformly to the whole S-2 region (Katayama, unpublished observation). Dr. Julian Davis, who worked with Harrington for many years, made similar observation as ours.

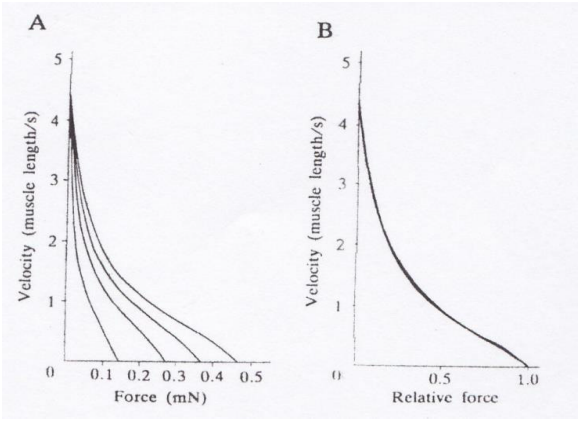

Figure 13: Effect of anti-S-2 antibody on the force-velocity curves of Ca^{2+}-activated muscle fibers, obtained at various steady isometric forces as shown in Figure 12. (A) The force-velocity curves obtained before (control) and at 30, 60 and 90 min after application of antibody (1.5 mg/ml). Note that the maximum shortening velocity under zero external loads, V_{max} remains constant despite marked time-dependent reduction. (B) The same force-velocity curves as in (A), normalized with respect to peak steady isometric forces. Note that the curves are identical [13].

Therefore, Harrington's antibody did not bind specifically to S-2 hinge region, but bound uniformly to the whole S-2 region. We will consider the surprising effect of the antibody on this basis.

The effect of anti-S-2 antibody, which attaches uniformly over the whole S-2 region, can be summarized as follows [13]: (1) It can reduce Ca^{2+}-activated isometric force to zero; (2) It can also reduce muscle fiber stiffness to zero; (3) Both force and stiffness decreases in parallel with each other; (4) Despite marked reduction of isometric force and muscle fiber stiffness, the maximum shortening velocity Vmax remains unchanged; (5) Despite marked reduction of isometric force and muscle fiber stiffness, MgATPase activity of muscle fiber does not change appreciably. Results (1), (2) and (3) can easily be explained as being due to decrease in the number of myosin heads producing isometric force, while result (5) indicates that myosin heads with the antibody attached can no longer participate in isometric force generation, but still hydrolyze ATP at the rate similar to that of native myosin heads. According to the dogma of Lymn-Taylor Scheme, however, myosin heads should hydrolyze ATP by repeating weak to strong actin binding transition. Result (4) obviously contradicts this dogma, since the strong myosin head binding to actin should produce internal resistance against muscle fiber shortening to result in decrease of Vmax.

Then, the question arises why myosin heads of antibody-attached myosin molecules do not produce internal resistance against muscle fiber shortening, while they repeat cyclic attachment-detachment with actin filaments, which has been believed to be coupled with the weak to strong actin-myosin binding transition? The puzzling question can only be accounted for by assuming that, when anti-S-2 antibody attaches to myosin molecules, their myosin heads no longer bind strongly to actin, but still hydrolyze ATP at the rate similar to that of myosin heads in native myosin molecules; myosin heads weakly binding with actin may readily be detached from actin with small vibrations applied to muscle fibers and also with myofilament sliding caused by a limited number of myosin heads in myosin molecules, which remain unbound with the antibody. The above explanation implies that, contrary to the generally believed dogma, ATP hydrolysis by myosin heads goes on without formation of strong actin-myosin binding. At present, we have no definite idea concerning the mechanism with which communication

is transmitted from myosin S-2 region to myosin head-actin interface. Much more experimental work is necessary to reach full understanding about the regulation of actin-myosin binding by myosin S-2 region.

Effect of p-phenylene dimaleimide on contraction characteristics and MgATPase activity of skinned muscle fibers

In 1986, we studied the effect of p-PDM, which binds with reactive sulfydrils in myosin head distal region to produce loss of its ability to bind with actin filament and to hydrolyze ATP [14], on contraction characteristics and MgATPase activity of skinned muscle fibers [15] with the following results: (1) Three different species of myosin molecules are present as a result of partial p-PDM modification, i.e. two head native-, one head inactivated-, and two head inactivated-myosin molecules, and their fractions to the total myosin molecules can be obtained by simple probabilistic calculation based on the total fraction of p-PDM-inactivated myosin heads, [14] (Figure 14). (2) Isometric force is only produced by two head native-myosin molecules, since the force is proportional to the square of (1-q) (Figure 15, left); (3) Mg ATPase activity is produced by both two head native- and one head native- (i.e. one head inactivated)- myosin molecules, since it is proportional to (1-q); and (4) One head native myosin molecules contribute not only to Mg ATPase activity, but also to internal resistance against muscle fiber shortening, as evidenced by the decrease of V_{max} with decreasing isometric force (Figure 15, right); (5) Two head inactivated-myosin molecules do not contribute to both muscle fiber stiffness and internal resistance against fiber shortening, being consistent with the result of HMM solution experiments [14]. Result (4) indicates that, in one head native-myosin molecules can hydrolyze ATP at the normal rate, but cannot produce force (and shortening) by some steric hindrance caused by inactivated head in the same molecule. In this case, native myosin heads in one head inactivated-myosin molecules hydrolyze ATP passing through the weak to strong actin-binding transition, which is no longer coupled with power stroke.

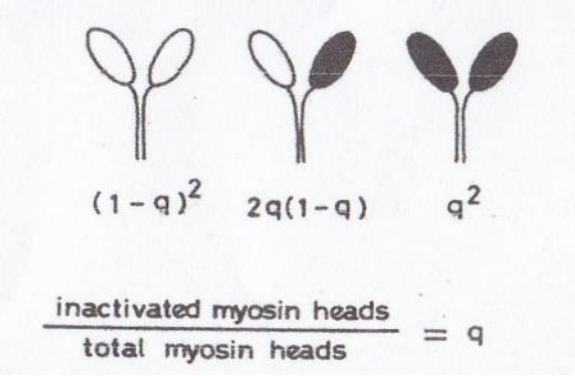

Figure 14: Three different species of myosin molecules and their respective fractions expressed by the total fraction of p-PDM-inactivated myosin heads, q, calculated by assuming independent reaction of two myosin heads in the same myosin molecule with p-PDM. Open and filled heads represent native and p-PDM- inactivated heads, respectively [15].

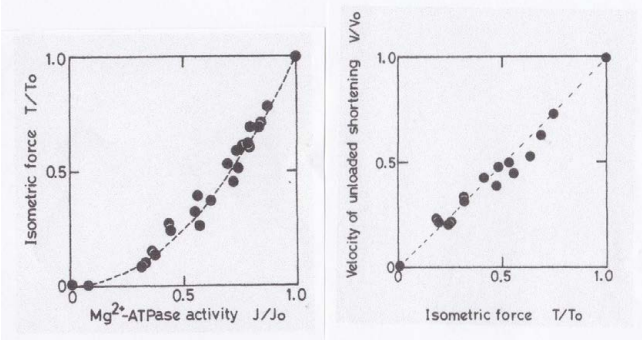

Figure 15: (Left) Relation between Mg ATPase activity and Ca^{2+}-activated isometric force. Note that isometric force is proportional to the square of total fraction of native myosin head, $(1-q)^2$. (Right) Relation between Ca^{2+}-activated isometric force and the maximum velocity of muscle fiber shortening V_{max}, measured by the slack test method. Note: V_{max} decreases with decreasing isometric force. Values of isometric force, Mg ATPase activity and V_{max} are expressed relative to control values [15].

Further evidence for the regulation of actin-myosin binding strength by myosin S-2 obtained from in vitro motility assay experiments

To obtain further evidence for the regulation of actin-myosin binding strength by myosin S-2 region, we constructed an in vitro force-movement assay system by using a centrifuge microscope [16]. As illustrated in Figure 16, the centrifuge microscope consisted of a rotor and a stroboscopic device to observe and video-record ATP-dependent movement of myosin-coated polystyrene beads along well-organized actin filament arrays (actin cables) in a giant algal cell, which were mounted in a cuvette fixed on the rotor. Without application of centrifugal force, beads exhibit ATP-dependent movement along actin cables with a constant velocity irrespective of whether they are coated with untreated myosin (control beads) or coated with myosin previously treated with anti-S-2 antibody (1 mg/ml). This result seems to correspond to the result that Vmax of muscle fiber remains unchanged despite marked reduction of isometric force (Figure 13). If centrifugal force is applied to the moving beads in the direction opposite to that of bead movement, the velocity of bead movement decreases with increasing centrifugal force, which serve as external load to the moving beads. The magnitude of centrifugal force required to stop and detach the moving beads are much larger for control beads (10.2 ± 4.8 pN, mean ± SD, n=8) than beads coated with antibody-treated myosin (1.1 ± 0.8 pN, n=7) [17]. This result constitutes additional evidence for the regulation of actin-myosin binding strength by myosin S-2 region.

Shortcomings of the swinging lever arm hypothesis

At the end of this review article, we will explain how the swinging lever arm hypothesis has been constructed, together with its shortcomings, As illustrated in Figure 17, a myosin head is like a tadpole in shape, consisting of oval shaped catalytic domain (CAD) and rod-like lever arm domain (LD), connected via small converter domain (COD). The LD is further connected to myosin filament backbone via myosin S-2 (not shown). Rayment et al. [18,19] prepared crystal of truncated myosin head (myosin S-1, obtained from slime mold *Dictyostellium*), in which most LD domain has been removed except for its base, and studied nucleotide-dependent structural changes in the myosin head crystal. Since it is not possible to actually bind nucleotides, ADP and ATP, to crystals, they used inorganic compounds as analogs of ADP and ATP. The nucleotide-dependent structural changes in the truncated myosin head were studied intensively by a number of investigators [20-22]. In addition to localized nucleotide-dependent structural changes around the nucleotide-binding cite in the CAD, they found that the base of the LD remaining in the truncated myosin exhibited rotation by ~60°. This rotation of the remaining LD base was taken to represent pre- and post-power stroke states of myosin head,

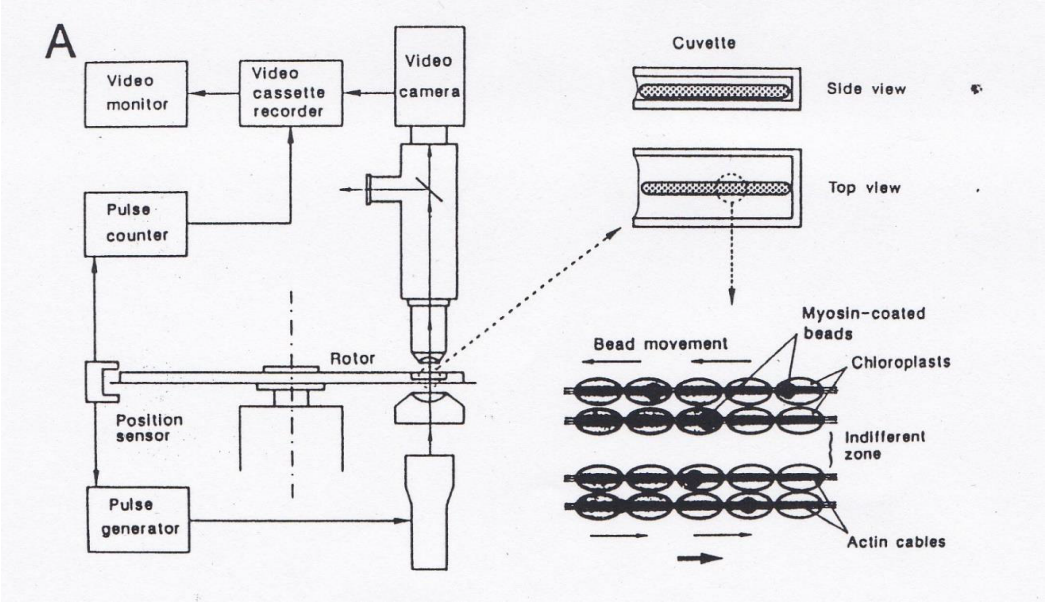

Figure 16: Diagram illustrating the centrifuge microscope to stroboscopically record ATP-dependent sliding of myosin-coated polystyrene beads along well organized actin filament arrays in a giant algal cell, which are mounted in the cuvette, fixed on the rotor of centrifuge microscope [16].

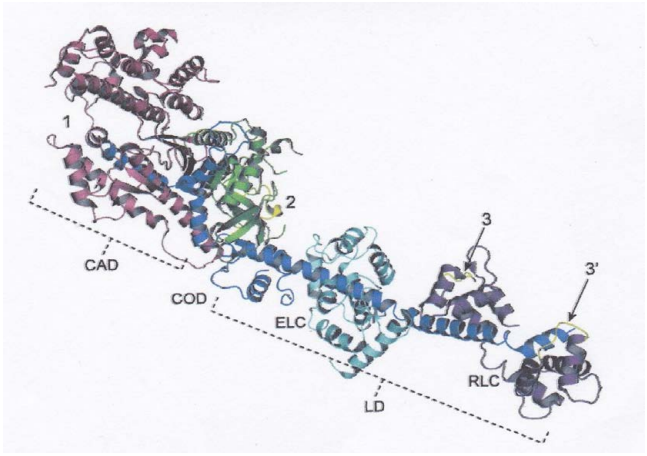

Figure 17: Structure of myosin head consisting of CAD, COD and LD domains. LD domain is further connected to myosin S-2 (not shown) extending from myosin filament backbone [25].

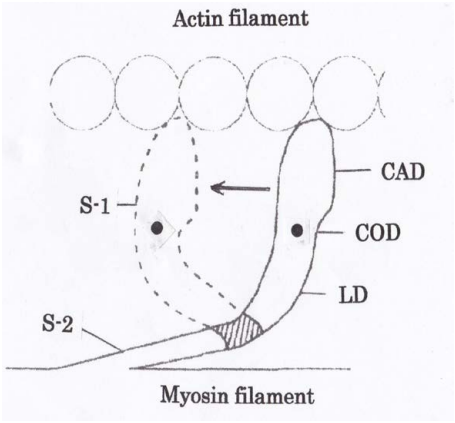

Figure 18: Diagram showing changes in myosin head configuration during power stroke while attached to actin filament. Myosin head CAD, COD, and LD domains are indicated by characters CAD, COD and LD, respectively. Filled circles in COD indicate approximate position of pivot, around which active rotation is assumed to take place. Shaded area shows junctional area between myosin head LD and myosin S-2. The change in angle between LD and S-2 around the junctional area is assumed to be passive in the swinging lever arm hypothesis.

assuming that the same rotation occurs if the whole LD is connected to truncated myosin. The above rather bold assumption indicates that the amplitude of rotation of at distal region of whole LD is enough to produce myosin power stroke in the direction parallel to myosin filament axis. Figure 18 is a diagram illustrating myosin head power and recovery strokes caused by active rotation of the CAD around the COD, as postulated by the swinging lever arm hypothesis.

Although the swinging lever arm hypothesis is now cited in every textbook as if it is an established fact, there are several shortcomings in the course of constructing this hypothesis. (1) To construct this theory, crystals of slime mold myosin was used instead of vertebrate skeletal muscle myosin because of the easiness to prepare crystals. Rather surprisingly, myosin head crystal structures were almost the same between slime mold and vertebrates despite the fact that slime mold differs so far from vertebrate animals. It seems possible that, due to close packing of myosin heads arising from crystal formation, functionally important differences in crystal structure between the two animals might be eliminated. (2) It is not well proved that the inorganic compounds used are actually good analogs of ADP and ATP. (3) Validity of the bold assumption to postulate rotation of the whole LD, based on the observed rotation of the remaining LD base in truncated myosin head is unclear. It seems rather unlikely that the small structures in the COD region can generate torque enough to produce myosin head power stroke in the myofilament-lattice, on which large external loads are imposed. The assumption that small structures in the COD region can actively rotate massive COD and CAD, with large loads applied to them, reminds me of an idiom, "The tail swings the dog". Such phenomena may take place in isolated molecules in solution, but

are unlikely to occur in the 3D myofilament-lattice supporting large external loads. (4) It can be seen in Figure 18 that, during power and recovery strokes, change in angle takes place not only at the CAD-LD junction, but also at the LD-S-2 junction. We do not understand the reason why the angle change at the LD-S-2 junction can be regarded to be passive in nature. (5) In constructing the swinging lever arm hypothesis, crystallographists appeared to pay no attention to possible role of S-2 region in producing myosin head movement, and ignored extensive work made by Harrington et al. though they published papers in mainstream journals, which do not allow one to make an excuse to overlook them. We reserve further comment about the issues stated above.

Meanwhile, Muhlrad et al. [23] reported that chemical modification (trinitrophenylation) of reactive lysine residue in myosin head COD eliminated ATP-dependent in vito actin-myosin sliding and actin-activated MgATPase activity. They interpreted these results as being due to mechanical collision of structures in the COD to result in the loss of lever arm rotation around the COD. Contrary to their report, however, we found that a monoclonal antibody attaching around reactive lysine residue in the COD [24] had no effect on Ca^{2+}-activated muscle contraction, while the antibody eliminated ATP-dependent in vitro actin-myosin sliding [25]. Generally speaking, binding of antibody to its epitope is reversible, while chemical modification is irreversible and may cause structural changes around the chemically modified region. Therefore, the report of Muhlrad et al. may not necessarily support the swinging lever arm mechanism, while our work may be taken to preclude it.

Conclusion

In this short review article, we presented evidence for the essential role of myosin S-2 region, which connect myosin heads to myosin filament backbone, especially its ability to regulate actin-myosin binding strength. At present, it is a mystery how myosin-S-2 transmit information to the actin-myosin interface at the distal region of myosin head CAD. In this article, we have also shown that the dogma in the Lymn-Taylor scheme is no longer valid: cyclic actin-myosin interaction coupled with ATP hydrolysis can take place in muscle without strong myosin head-actin binding when anti-S-2 antibody binds with S-2 region. In general, we hope muscle investigators, especially young ones, to realize that textbook view is convenient but not necessarily reliable, and start challenging a number of mysteries still remaining in the molecular mechanism of muscle contraction.

Acknowledgements

We wish to dedicate this article to the late Professor William F Harrington, who worked with us using the antibody prepared in his laboratory.

References

1. Huxley H, Hanson J (1943) Changes in the cross-striations of muscle during contraction and stretch and their structural interpretation. Acta Physiol Scani 6: 123.
2. Huxley HE (1969) The mechanism of muscular contraction. Science 164: 1356-1365.
3. Huxley HE (1953) Electron microscope studies of the organization of the filaments in striated muscle. Biochimica et Biophysica Acta 12: 387-394.
4. Bagshaw CR (1982) Mechanism of ATP hydrolysis. Muscle Contraction, pp. 39-46.
5. Lymn RW, Taylor EW (1971) Mechanism of adenosine triphosphate hydrolysis by actomyosin. Biochemistry 10: 4617-4624.
6. Sugi H, Akimoto T, Sutoh K, Chaen S, Oishi N, et al. (1997) Dynamic electron microscopy of ATP-induced myosin head movement in living muscle thick filaments. Proceedings of the National Academy of Sciences 94: 4378-4382.
7. Ueno H, Harrington WF (1986) Local melting in the subfragment-2 region of myosin in activated muscle and its correlation with contractile force. Journal of Molecular Biology 190: 69-82.
8. Sugi H, Minoda H, Inayoshi Y, Yumoto F, Miyakawa T, et al. (2008) Direct demonstration of the cross-bridge recovery stroke in muscle thick filaments in aqueous solution by using the hydration chamber. Proceedings of the National Academy of Sciences 105: 17396-17401.
9. Sugi H, Chaen S, Akimoto T, Minoda H, Miyakawa T, et al. (2015). Electron microscopic recording of myosin head power stroke in hydrated myosin filaments. Scientific reports 5: 15700.
10. Huxley AF (1957) Muscle structures and theories of contraction. Progr Biophys Chem 7: 255-318.
11. Lovell S, Karr T, Harrington WF (1988) Suppression of contractile force in muscle fibers by antibody to myosin sub fragment 2. Proceedings of the National Academy of Sciences 85: 1849-1853.
12. Harrington WF, Karr T, Busa WB, Lovell SJ (1990) Contraction of myofibrils in the presence of antibodies to myosin subfragment 2. Proceedings of the National Academy of Sciences 87: 7453-7456.
13. Sugi H, Kobayashi T, Gross T, Noguchi K, Karr T, et al. (1992) Contraction characteristics and ATPase activity of skeletal muscle fibers in the presence of antibody to myosin sub fragment 2. Proceedings of the National Academy of Sciences 89: 6134-6137.
14. Reisler E (1980) On the question of co-operative interaction of myosin heads with F-actin in the presence of ATP. Journal of molecular biology 138: 93-107.
15. Chaen S, Shimada M, Sugi H (1986) Evidence for cooperative interactions of myosin heads with thin filament in the force generation of vertebrate skeletal muscle fibers. J Bio Chem 261: 13632-13636.
16. Oiwa K, Chaen S, Kamitsubo E, Shimmen T, Sugi H (1990) Steady-state force-velocity relation in the ATP-dependent sliding movement of myosin-coated beads on actin cables in vitro studied with a centrifuge microscope. Proceedings of the National Academy of Sciences 87: 7893-7897.
17. Tsuchiya T, Tanaka H, Shirakawa I, Karr T, Sugi H (1998) Evidence for the essential role of myosin subfragment-2 in the ATP-dependent actin-myosin sliding in muscle contraction. The Japanese Journal of Physiology 48: 383-387.
18. Rayment I, Rypniewski WR, Schmidt-Bäse K, Smith R, Tomchick DR, et al. (1993) Three-dimensional structure of myosin subfragment-1: A molecular motor. Science 50-58.
19. Rayment I, Holden HM, Whittaker M, Yohn CB, Lorenz M, et al. (1993) Structure of the actin-myosin complex and its implications for muscle contraction. Science-New York Then Washington 261: 58-58.
20. Geeves MA, Holmes KC (1999) Structural mechanism of muscle contraction. Annual review of biochemistry 68: 687-728.
21. Geeves MA, Holmes KC (2005) The molecular mechanism of muscle contraction. Advances in protein chemistry 71: 161-193.
22. Sweeney HL, Houdusse A (2010) Structural and functional insights into the myosin motor mechanism. Annual review of biophysics 39: 539-557.
23. Muhlrad A, Peyser YM, Nili M, Ajtai K, Reisler E, et al. (2003) Chemical decoupling of ATPase activation and force production from the contractile cycle in myosin by steric hindrance of lever-arm movement. Biophysical journal 84: 1047-1056.
24. Sutoh K, Tokunaga M, Wakabayashi T (1989) Electron microscopic mappings of myosin head with site-directed antibodies. Journal of molecular biology 206: 357-363.
25. Sugi H, Chaen S, Kobayashi T, Abe T, Kimura K, et al. (2014) Definite differences between in vitro actin-myosin sliding and muscle contraction as revealed using antibodies to myosin head. PloS one 9: 93272.